

## A statistical analysis of wind speed data using Burr, generalized gamma, and Weibull distributions in Antakya, Turkey

İlker MERT<sup>1</sup>, Cuma KARAKUŞ<sup>2,\*</sup>

<sup>1</sup>Maritime Vocational School, Mustafa Kemal University, Hatay, Turkey

<sup>2</sup>Department of Mechanical Engineering, Mustafa Kemal University, Hatay, Turkey

Received: 07.02.2014

Accepted/Published Online: 15.07.2014

Printed: 30.11.2015

**Abstract:** The wind energy potential of the Antakya area was statistically analyzed based 8 years of wind data sets (2002–2009). The 4-parameter Burr, 3-parameter generalized gamma, and conventional Weibull distributions were regarded as suitable statistical models for describing wind speed profiles. The suitability of the models was tested by  $R^2$ ,  $RMSE$ , chi-squared, and Kolmogorov–Smirnov analysis. According to goodness-of-fit tests, the Burr distribution was found to be more suitable than the generalized gamma or Weibull distributions for representing the actual probability of wind speed data for Antakya. Based on the capacity factors estimated by the Burr model at a hub height, the power generation potential of a commercial 330-kW wind turbine was also determined. The results show that the available wind energy potential to generate electricity in Antakya is low; consequently, wind power would be suitable only for stand-alone electrical and mechanical applications, such as water pumps, battery charging units, and local consumption in off-grid areas.

**Key words:** Wind energy, 4-parameter Burr, 3-parameter generalized gamma, Weibull, energy harvesting

### 1. Introduction

Wind energy is quickly becoming preferred as an economical energy source around the world, with competitive investors and progress in wind energy technologies over the last 3 decades [1]. Today, more than 1 billion people, or 18% of the population worldwide, do not have access to grid electricity [2]. Hence, wind energy has the advantage of being suitable for rural and remote regions. Turkey is challenged by a rapidly growing economy, an expanding population, and a growing power demand. The country has been among the 4 fastest developing energy markets around the world for the last 3 decades [3]. The wind energy sector has made rapid progress and its capacity has increased from 146.25 MW in 2007 to 2089 MW in 2012, while the installed wind power capacity in the European Union grew from 57 GW in 2007 to 100 GW in 2012 [4]. While the installed capacity in Europe has increased by about 75%, Turkey's capacity has increased 13.3-fold (1330%) over the same period. Turkey possesses excellent wind resources, particularly in the Çanakkale, İzmir, Balıkesir, and Hatay regions. Depending on the geographical position and seasonal influences, Turkey's total feasible wind energy potential has been reported by the Republic of Turkey Ministry of Energy and Natural Resources to vary between 5000 and 48,000 MW, and this situation has been providing significant growth for the Turkish wind market over the coming years [5]. In the Hatay basins, the highest monthly wind speed value is 25.5 m/s and the annual average wind energy potential is 25–50 W/m<sup>2</sup>. In 2012, the electricity generated from the annual wind power in the

\*Correspondence: ckarakus@mku.edu.tr

Hatay region was 156 GWh (for an equivalent of 2500 hours of full load/year) [6]. As of 2013, the presently established power lines in that basin have a capacity of 177.50 MW, plus an additional 253 MW currently under construction [7]. Determining wind characteristics is necessary for estimating wind resources so that reasonable decisions can be made regarding the technical and economic feasibility of any power plant generating electricity from wind. In the last 15 years, many studies have been carried out to determine the wind profile and the potential in Turkey and in many other countries. Moreover, wind speed was modeled by different probability density functions in these studies. Sahin et al. investigated wind characteristics and wind potential using the Weibull distribution in the Antakya and İskenderun regions of Hatay in Turkey [8]. It was concluded that the rates of wind energy potential in both regions were adequate to generate electricity, thanks to the prevailing southwesterly winds in the Antakya region. Sahin and Bilgili also researched the wind profile of the Belen region of Hatay in Turkey using hourly wind speed and direction data for 2 years (2004–2005) [9]. That study showed that Belen is a suitable area for wind energy. Similarly, Celik analyzed the acceptability of the Weibull and Rayleigh distributions for modeling local wind profiles. Their parameters were based on 12 months of wind speed and direction data recorded in the İskenderun region of Hatay in Turkey [10]. The Weibull distribution proved accurate throughout Celik's study and was more suitable than the Rayleigh distribution. However, the effects of seasonal and monthly climates can change the degree of suitability of any distribution function [11]. In another study, Gökçek et al. investigated the wind profile of the Kırklareli region in Turkey in order to determine the energy potential that was attainable via use of wind for energy generation [12]. These researchers found that the annual mean power density for this region (as calculated based on the Weibull distribution parameters) was  $138.85 \text{ W/m}^2$ . Gökçeada Island (northern Aegean Sea, Turkey) is another windy area investigated by Eskin et al. using wind speed and direction data recorded at a height above ground level (HAGL) of 10–30 m [13]. This study showed that Gökçeada Island has high wind energy ( $500 \text{ W/m}^2$  at 25 m HAGL) due to atmospheric stability and high wind speeds. In terms of statistical analysis and modeling, wind speed and wind energy studies are very limited in Antakya. Therefore, the objective of this study was to determine the wind energy potential in Antakya through the use of a variety of statistical distributions, including the Burr, generalized gamma, and Weibull distributions.

## 2. Site and measurement details

The shores of Turkey along the eastern Mediterranean are suitable for wind power generation and therefore are the most attractive regions for the construction of wind power plants. Antakya is the capital city of Hatay Province, which is located in the eastern end of the Mediterranean Sea and within the border region of Turkey, as seen in Figure 1. It is located at  $35^\circ 52' - 37^\circ 04' \text{N}$  and  $35^\circ 40' - 36^\circ 35' \text{E}$ , with  $5403 \text{ km}^2$  of surface area. The coordinates of the Antakya meteorological observation station are  $36^\circ 12' \text{N}$ ,  $36^\circ 9' \text{E}$ . All observations at the meteorological station were measured using pressure and temperature sensors and an anemometer with 3 cups (at 10 m HAGL). Instantaneous wind data measured at Antakya meteorological station were recorded as the average of 60 min of data and transmitted to the Turkish State Meteorological Service (TSMS) from January 2002 to December 2009. These values obtained from TSMS have been quality-assured for this study. Statistical software applications were used to assess the data obtained for the wind speed and the direction data.

### 2.1. Method

In the literature about wind energy, several methods have been proposed to estimate wind energy potential. Statistical analyses are commonly used to describe wind profile based on a Weibull function. In our study, the

4-parameter Burr and 3-parameter generalized gamma functions were tested as new models for wind speed. At the end of the study, both estimated wind power densities and statistical errors of probability models were also compared.



Figure 1. The map of the region (Maphill, 2011).

## 2.2. Wind speed data

To evaluate the wind potential of any point requires precise identification of wind speed frequency distribution. When the wind characteristics, and in particular the speed frequency distribution, are exactly known, the wind power potentiality and the economic feasibility of a given wind power application of any size can be easily estimated for the regions of interest [14]. Therefore, determination of wind speed variability is usually the initial focus in order to define a suitable distribution for wind speed. Mean wind speed (MWS) denotes the suitability of a windy area for electricity generation from wind. MWS, or  $V_m$  (m/s), of a region is defined in

Eq. (1) for the available time series data. Thus, all MWS values (daily, monthly and annual) were calculated with Eq. (1)

$$V_m = \frac{1}{N} \sum_i^N V_i, \quad (1)$$

where  $V_i$  is the wind speed value at time  $i$  and  $N$  is the number of times wind speed was measured. In this study, the wind speed data were collected at an observation height  $H_{obs}$  [m] that was different from the hub height. The direct measurements at 10 m HAGL can be representative for small or micro wind turbines; larger wind turbines have a hub height of around 50–100 m [15]. Therefore, it is necessary to determine the relationship among wind speed  $V_{hub}$  [m/s] at hub height  $H_{hub}$  [m], the wind speed  $V_{obs}$  [m/s] at  $H_{obs}$ , and the surface roughness length  $Z_0$  [m]. Hensen reported that the logarithmic law could be used to extrapolate the wind speed because it is based on physical laws rather than on an empirical formulation [16]. For this study, the logarithmic law was proposed as a relation given by Eq. (2) [17]:

$$V_{hub} = V_{obs} \left[ \frac{\ln \frac{H_{hub}}{Z_0}}{\ln \frac{H_{obs}}{Z_0}} \right], \quad (2)$$

where  $Z_0$  was assumed to be 0.8 since the mast is located in an urban area [18].

On the other hand, calculation of average power output for a wind turbine is proportional to air density and requires the measurement of air density  $\rho$  [kg/m<sup>3</sup>] [19].

Air density depends essentially on pressure and temperature, and air density can be calculated using the ideal gas law [20]. Air density is given as:

$$\rho = p \div (R_d \times T), \quad (3)$$

where  $p$  is the air pressure [Pa],  $T$  is the temperature in degrees Kelvin [K], and  $R_d$  is the universal gas constant of dry air [287 j/kg K].

### 2.3. Statistical analysis methodology

After the calculation of the MWSs, several distributions could possibly be used with the help of the calculation of general wind parameters. The distributions that are used most often (and are most readily recognized) are the Weibull, Burr, and generalized gamma distributions. In this study, each of these distributions was examined for its ability (or lack thereof) to model wind speed frequency distributions in the Antakya region. Commonly used methods are the moments method, the least squares method, the power density method, and the method of maximum likelihood estimation (MLE) when determining the parameters of a distribution function [21,22]. In all cases, during this study, the parameters of the theoretical distributions were estimated using the MLE method, one of the most efficient methods for this purpose [23]. The method for a fixed set of data and an underlying statistical distribution selects values for the distribution parameters that maximize the likelihood function. In addition, the MLE method supplies forecasts with favorable properties; that is, the forecasts are asymptotically centered, have normal asymptotic distribution, and are efficient [24]. According to some researchers, the Weibull function is the best for modeling the wind speed [25,26]. However, Hennessey, Aidan, and Ododo have expressed that the Weibull function does not model the wind speed well for regions having very low or calm wind speeds [27,28]. Therefore, in this study, the 4-parameter Burr function was also studied. The

Weibull probability distribution function has been extensively used in wind energy applications and is defined by the following equation:

$$f(x) = \frac{k}{c} \left[ \frac{V}{c} \right]^{k-1} e^{-\left(\frac{V}{c}\right)^k}, \quad (4)$$

where  $k$  is the dimensionless shape parameter and  $c$  the scale parameter in m/s.  $k$  and  $c$  can be estimated by using MLE [29,30]. The Burr distribution has a flexible form and it is considered a natural rival to normal distribution for statistical modeling. In particular, the controllable scale and location parameters of the Burr distribution make it appealing for fitting wind speed data and plotting a slightly positive skewness [31]. Valerio et al. applied the Burr model to wind data collected in an urban area and their findings show that the Burr model had a better congruity concerning the accuracy of fitting the empirical data [32]. The probability density function of the Burr distribution is given by the following equation:

$$f(x) = \alpha k \left( \frac{V - \gamma}{\beta} \right)^{\alpha-1} \div \beta \left( 1 + \left( \frac{V - \gamma}{\beta} \right)^\alpha \right)^{k+1}; \gamma \leq V < +\infty, \quad (5)$$

where  $\beta$  is the scale parameter in m/s,  $k$  and  $\alpha$  are the dimensionless shape parameters, and  $\gamma$  is the location parameter [33]. Among the 3 distribution models used in this study, the 3-parameter generalized gamma distribution function was accepted as another useful model. Auwera et al. investigated the use of the 3-parameter generalized gamma distribution to describe wind speed distributions [34]. Moreover, the generalized gamma distribution provided better results in fitting the measured wind speed distribution than a number of other distribution functions in this study. The generalized gamma distribution is also parameterized in terms of 2 shape parameters ( $k - \alpha$ ). The scale parameter  $\beta$  is defined by Eq. (6):

$$f(x) = \frac{kV^{k\alpha-1}}{\beta^{k\alpha}\Gamma(\alpha)} \exp(-(V/\beta)^k). \quad (6)$$

In order to assess the goodness-of-fit of the applied distribution models, the  $K - S$  and chi-squared statistical tests were used after stacked/unstacked negative and 0 wind speed values were eliminated. These tests measure the suitability of an applied theoretical probability distribution function for a random sample of wind speed values; that is, they indicate how well the distribution fits the existing wind speed data. However, the 2 tests can produce different results due to the different analytical structures. The result of the chi-squared test statistic is affected by bin changes. On the other hand, the  $K - S$  test is based on the empirical cumulative distribution function (CDF) and is contrasted with the empirical distribution function of the data; thus, it is sensitive to extreme values [35]. However, since the  $K - S$  and chi-squared tests are commonly used ones, these tests have been conducted as the first selection procedure. As the second procedure,  $RMSE$  and  $R^2$  values were calculated between prediction and observation to make the best possible assessment. The definitions of these statistics can be seen in Table 1:  $K$  is the number of bins,  $N$  is the total number of observations, and  $O_i$  and  $E_i$  are observed and estimated frequencies for bin I, respectively. Furthermore,  $Y_i$  represents the  $i$ th entry of measured data while  $F$  is the cumulative distribution function. Estimated, observed, and mean values are denoted by  $x_i$ ,  $y_i$ , and  $y^*$ , respectively, if equations of the  $R^2$  and  $RMSE$  are considered. In addition, the relative errors (in %) of estimated wind speed ( $P_e$ ) were calculated by the following equation:

$$Error(\%) = \left( \frac{P_e - P_o}{P_o} \right) 100\%. \quad (7)$$

**Table 1.** Goodness-of-fit statistics.

Statistic	Definition
<i>Chi-squared</i>	$\chi^2 = \sum_{i=1}^K \frac{(O_i - E_i)^2}{E_i}$
<i>K - S</i>	$D = \max(F(Y_i) - (i - 1)/N, i/N - F(Y_i))$
<i>RMSE</i>	$RMSE = (1 - \sum_{i=1}^n (y_i - x_i)^2)^{0.5}$
<i>R<sup>2</sup></i>	$R^2 = 1 - \left[ \left( \sum_{i=1}^N (y_i - x_i) \right) \div \left( \sum_{i=1}^N (y_i - \bar{y})^2 \right) \right]$

### 2.4. Wind power density

Calculation of wind power density is another step in assessing wind energy potential. Wind speed data measured over the 8-year period were employed to estimate the wind power density in the windy area of the Antakya region. The expected monthly or annual wind power density can be expressed by using Eq. (8):

$$P = (1/2)\rho V_m^3, \tag{8}$$

where  $\rho$ , which depends on altitude, air pressure, and temperature, is the mean air density and  $V_m^3$  is the third power of the MWS value. The Battelle Pacific Northwest Laboratory developed a wind power density classification table to classify wind resources; this table is reproduced in Table 2 [36]. In this table, wind power density classification ranges from Class 1 (the lowest) to Class 7 (the highest). Each class represents a range of wind power density [W/m<sup>2</sup>] or a range of equivalent MWSs at heights of 10 m and 50 m [37]. Class 1 and 2 areas are considered unsuitable and marginal for wind power development, respectively. In many cases, Class 3 and higher classes are considered to be useful for wind turbine generators of up to 750-kW rating.

**Table 2.** International commercial system of classification for wind power density.

Wind power class	Wind power density (W/m <sup>2</sup> ) and speed (m/s) 10 m	Wind power density (W/m <sup>2</sup> ) and speed (m/s) 50 m
1	≤ 100; ≤4.4	≤ 200; ≤5.6
2	≤ 150; ≤5.1	≤ 300; ≤6.4
3	≤ 200; ≤5.6	≤ 400; ≤7.0
4	≤ 250; ≤6.0	≤ 500; ≤7.5
5	≤ 300; ≤6.4	≤ 600; ≤8.0
6	≤ 400; ≤7.0	≤ 800; ≤8.8
7	≤ 1000; ≤9.4	≤ 2000; ≤11.9

### 2.5. Capacity factor and selecting wind turbine

Capacity factor ( $C_f$ ) is one parameter in measuring the productivity of a wind turbine.  $C_f$  compares how much electricity a wind turbine actually produces over a given period of time with the amount of power output for the wind turbine running at full capacity for the same amount of time.  $C_f$ , given by Eq. (9), can be expressed as a percentage [38].

$$C_f = WEP/WEP_{max}, \tag{9}$$



where  $WEP$  represents actual wind energy produced [Wh/year] by the wind turbine and  $WEP_{max}$  is the maximum wind energy that the wind turbine produces [Wh/year]. Additionally, annual electricity production (AEP) can be calculated by Eq. (10):

$$AEP = WEP \times T \quad (10)$$

where  $T$  is 8760 h. In this study, an Enercon 33 (rated power output is 330 kW at a wind speed of 13 m/s and a cut-in wind speed of 3.0 m/s) commercial wind turbine was used for estimating energy production. The turbine's power curve is given in Figure 2 [39].

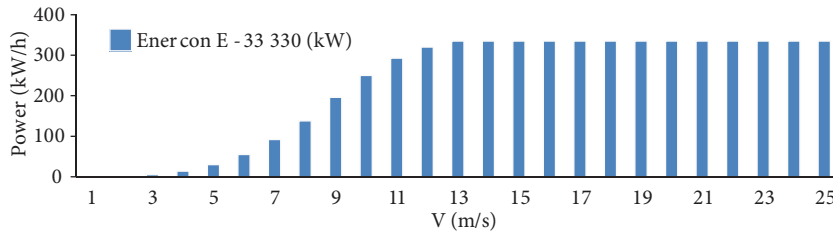


**Figure 2.** Power curve of wind turbine (model no. E-33, Enercon Ltd.).

### 3. Results

#### 3.1. Descriptive wind speed statistics

The annual MWS and standard deviations in the Antakya–Hatay region during the period from 2002 to 2009 are presented in Figure 3 and exhibit similar variations. As indicated over the entire 8-year period, the highest average hourly wind speed of 7.90 m/s was recorded in July 2003, while the lowest MWS of 0.10 m/s occurred in November 2009. The mean annual wind speed in the period from 2002 to 2009 was 2.59 m/s. The highest maximum wind speed occurred in 2008; it was 20.04 m/s west–southwest. The yearly wind characteristics, which were derived from the measurements of the wind speed data in the site from 2002 to 2009, are given in Table 3. Wind speed characteristics are critically important for the evaluation of the possibilities of wind power utility. This evaluation is usually achieved by the values given in Table 3. While mean speed varied from 2.39 m/s to 2.70 m/s, maximum hourly MWS was 7.90 m/s in 2003. Standard deviation, describing the amount of variability or dispersion around MWS data, varied between 1.52 m/s in 2009 and 1.71 m/s in 2006. Skewness (a measure for the degree of symmetry in a variable distribution) did not exceed 0.53. Kurtosis (a measure of the peakedness of wind speed distribution) varied from  $-0.82$  to  $-1.07$  for all periods. In order to construct the regional wind rose (the analysis of the frequency distribution based on yearly and seasonal wind speed data), all hourly average wind speed values and wind directions were used; these are given in Table 4. According to this table, wind directions behave similarly in spring and fall. The prevailing wind direction was south–southwest ( $86.01\%$ ) during the summer, while the prevailing wind direction was northeast ( $60.46\%$ ) during the winter. If annual wind speed data are taken into consideration, it is evident that the wind blows predominantly from the south–southwest ( $202.5^\circ$ ) about  $44\%$  of the time, and from the northeast ( $45^\circ$ ) about  $27.8\%$  of the time. However, in terms of power production, the summer is more suitable due to more energy-carrying winds. In addition, for the construction of wind turbines, minimally high buildings that exist in the investigated area should be considered, since the mast is located in an urban area ( $Z_0 \geq 0.8$ ).

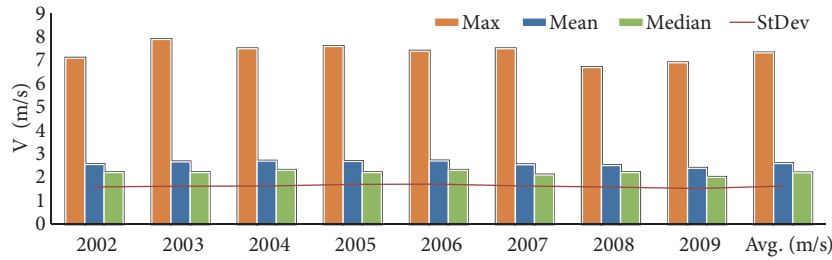


Figure 3. Annual MWS and standard deviations.

Table 3. Yearly wind speed characteristics.

Year	Mean	SD	Variance	Min	Max	Skewness	Kurtosis
2002	2.55	1.59	2.52	0.00	7.10	0.51	-0.86
2003	2.66	1.62	2.62	0.10	7.90	0.43	-0.98
2004	2.69	1.63	2.65	0.00	7.50	0.43	-0.92
2005	2.68	1.70	2.89	0.00	7.60	0.45	-1.00
2006	2.70	1.71	2.92	0.00	7.40	0.40	-1.07
2007	2.54	1.63	2.65	0.00	7.50	0.53	-0.82
2008	2.51	1.58	2.51	0.00	6.70	0.42	-0.99
2009	2.39	1.52	2.31	0.00	6.90	0.47	-0.88
Avg. (m/s)	2.59	1.62	2.63	0.01	7.33	0.46	-0.94

Table 4. Season and overall wind direction frequency.

	N	NNE	NE	ENE	E	ESE	SE	SSE	S	SSW	SW	WSW	W	WNW	NW	NNW
Winter	74	307	1306	126	11	5	3	9	10	132	41	52	9	7	11	57
Spring	36	120	550	112	9	2	3	1	26	952	218	89	20	11	15	44
Summer	3	10	14	6	2	1	2	0	16	1899	224	15	4	2	4	6
Autumn	43	135	571	65	7	7	2	4	14	871	261	114	46	13	3	28
Overall	156	572	2435	309	29	15	10	14	66	3854	744	270	79	33	33	133

### 3.2. Wind speed distribution fitting

Due to the changes in the local meteorological conditions and the random nature of the wind, estimating the behavior of wind speed is difficult. It is more practical to represent its behavior using a probability function; also, the seasonal variation of wind speed data can help in describing local wind profiles. Due to the skewness and kurtosis values over the 8 years of the study, it is clear that wind speed data in this study can be analyzed with distributions aside from the normal distribution. The reason is that these values are equal to 0 for normal distribution. Therefore, in this study, the Burr, generalized gamma, and Weibull distributions were used to determine the wind distribution that best describes the wind speed variation of Antakya. Monthly, seasonal, and annual variations for actual and estimated MWS, power density, and parameters of each distribution in Antakya at 10 and 50 m HAGL are listed in Tables 5–7. The Weibull parameter  $c$  varied between 1.42 m/s in December and 4.97 m/s in July, while  $k$  varied between 1.73 in May and 4.52 in August. The highest values of  $c$  and  $k$  were obtained in the summer, when the wind is usually regular with high speeds. The monthly generalized gamma shape parameter  $k$  varied between 0.90 m/s in July and 1.01 m/s in November. The highest value of  $k$  was 0.99 in winter and the highest values of  $\alpha$  and  $\beta$  were obtained in summer and autumn, respectively. For the Burr distribution, the  $k$  shape parameter varied between 707.67 in July and 5.80 in January, while the scale parameter  $\beta$  varied between 12.04 in August and 94.71 in April. The highest value of the other shape



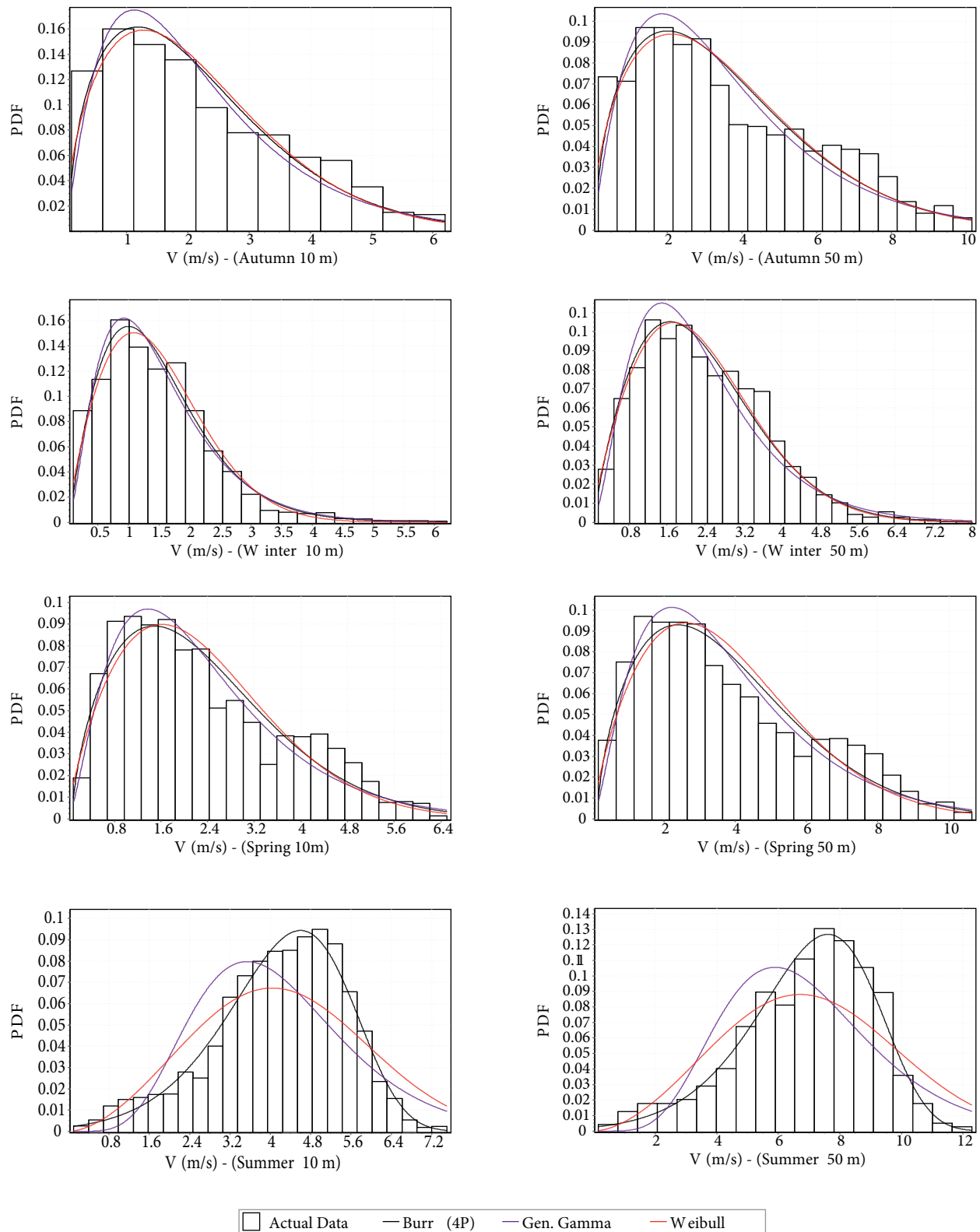
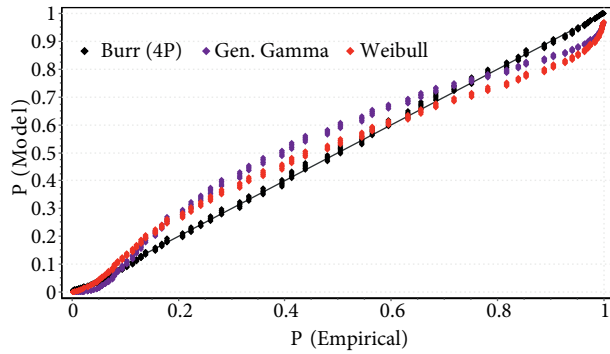
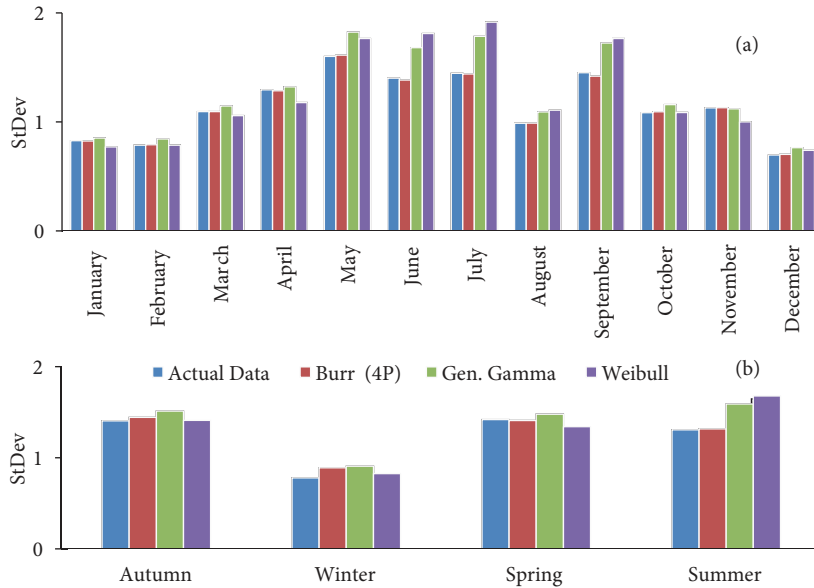


Figure 4. Seasonal histograms of the wind speed data.



**Figure 5.** Probability difference plots of the fitted Burr, generalized gamma, and Weibull models.



**Figure 6.** a) Monthly variation of SD. b) Seasonal variation of SD.

parameter  $\alpha$  was obtained during the summer. Height values of the  $\gamma$  parameter were observed in the spring while the Burr location parameter  $\gamma$  varied between  $-16.36$  in July and  $0.09$  in January. As seen in Table 6, average wind speeds estimated by the Burr, generalized gamma, and Weibull distributions were very close to real wind speeds. Table 6 also contains the monthly variation in mean actual wind power density (at 10 m HAGL) in Antakya. As can be seen in Table 7, the monthly mean power density was highest during summer and lowest during winter (at 10 m and 50 m HAGL). The mean wind power densities estimated by the Burr, generalized gamma, and Weibull distributions are very close to real mean wind power density values. However, both MWS and power density values, which were estimated by the Weibull distribution, were less successful. The highest mean power value was  $212.46 \text{ W/m}^2$  in August and the lowest mean power was  $5.38 \text{ W/m}^2$  in December at 50 m; therefore, Antakya is classified as a wind power density class 2 region ( $\leq 250 \text{ W/m}^2$ ). This means that the region is not suitable for large-scale wind energy convertor systems. In this study, probability density distributions derived from the measured hourly time series data versus those obtained from the Burr, generalized gamma, and Weibull models during seasonal periods at the site (at 10 m and 50 m HAGL) are illustrated in Figure 4. The Weibull model overpredicted wind speeds in May, June, July, and August, which were in the ranges of 3 to 5 m/s and 10 to 12 m/s, respectively. The generalized gamma model underpredicted

**Table 5.** Monthly, seasonal, and annual variations for parameters of distributions.

Month	Burr parameters				Gen. gamma parameters			Weibull parameters	
	$k$	$\alpha$	$\beta$	$\gamma$	$k$	$\alpha$	$\beta$	$k$	$c$
January	5.80	1.82	17.38	0.09	0.98	3.30	0.45	2.05	1.70
February	524.96	1.83	47.87	0.05	0.96	3.17	0.43	1.90	1.62
March	173.82	1.75	39.31	0.05	0.97	2.92	0.63	1.86	2.13
April	414.02	1.61	94.71	0.09	0.99	2.61	0.80	1.83	2.34
May	567.75	1.94	88.63	-0.06	0.92	3.02	0.87	1.73	3.32
June	253.56	5.95	19.34	-3.12	0.91	6.57	0.50	2.37	4.56
July	707.67	17.75	30.84	-16.36	0.90	7.12	0.49	2.46	4.97
August	68.77	8.19	12.04	-2.38	0.96	17.55	0.22	4.52	4.83
September	344.70	3.33	27.62	-1.13	0.91	3.98	0.67	1.89	3.61
October	537.33	1.72	78.92	0.05	0.96	2.80	2.80	1.77	2.09
November	24.78	1.36	16.64	0.08	1.01	1.90	0.82	1.55	1.69
December	259.30	1.86	28.14	0.00	0.94	3.01	0.39	1.77	1.42
Winter	7.43	1.83	4.55	0.04	0.99	2.73	0.53	1.85	1.66
Spring	510.41	1.64	113.15	0.08	0.97	2.62	0.85	1.77	2.59
Summer	510.41	9.24	19.45	-5.98	0.92	8.13	0.42	1.85	1.66
Autumn	894.82	1.49	221.27	0.06	0.95	2.27	0.91	1.57	2.42
Annual	1141.10	1.51	293.76	0.07	0.95	2.28	1.04	1.58	2.81

**Table 6.** Actual-estimated MWS and power densities.

Month	Observed MWS [m/s] and power density 10 m		Estimated MWS [m/s] 50 m			
	$V_{Obs}$	$P_{Obs}$	$V_{Obs}$	$V_{Burr}$	$V_{GGamma}$	$V_{Wei}$
January	1.52	2.18	2.49	2.50	2.49	2.47
February	1.44	1.84	2.36	2.37	2.36	2.36
March	1.91	4.19	3.12	3.12	3.11	3.10
April	2.11	5.60	3.45	3.46	3.45	3.40
May	2.94	14.98	4.81	4.82	4.79	4.85
June	3.95	35.69	6.46	6.47	6.44	6.62
July	4.31	46.11	7.06	7.07	7.04	7.22
August	4.39	48.41	7.19	7.20	7.19	7.22
September	3.13	17.81	5.13	5.16	5.11	5.24
October	1.87	3.84	3.06	3.06	3.04	3.05
November	1.55	2.26	2.54	2.54	2.54	2.49
December	1.26	1.23	2.06	2.06	2.05	2.07
Winter	1.41	1.71	2.30	2.42	2.42	2.41
Spring	2.32	7.47	3.80	3.80	3.80	3.77
Summer	4.22	43.26	6.91	6.84	6.82	6.95
Autumn	2.18	6.13	3.57	3.57	3.55	3.55
Annual	2.54	9.74	4.16	4.16	4.14	4.13
Relative Mean Error				0.46%	0.62%	1.17%

data by 7 to 9 m/s. This is reflected by the underestimated probabilities in the summer, as seen in Figure 4. However, the same figure indicates that the Burr model performed better than the generalized gamma and Weibull models in all periods. In addition, the probability plot used to test whether the empirical CDF values

**Table 7.** Variations for estimated mean power density of distributions (at 50 m).

Month	Estimated power density [W/m <sup>2</sup> ] 50 m			
	$P_{Obs}$	$P_{Burr}$	$P_{Gamma}$	$P_{Wei}$
January	9.56	9.59	9.53	9.30
February	8.10	8.11	8.02	8.03
March	18.40	18.41	18.26	18.08
April	24.59	24.70	24.58	23.53
May	65.75	65.89	64.74	67.13
June	156.62	157.47	155.18	168.19
July	202.35	203.15	200.70	216.30
August	212.46	212.92	212.06	214.61
September	78.15	79.19	76.96	83.25
October	16.86	16.91	16.68	16.75
November	9.92	9.90	9.97	9.35
December	5.38	5.38	5.30	5.47
Winter	7.52	8.77	8.74	8.58
Spring	32.77	32.85	32.70	31.97
Summer	189.84	184.22	182.48	193.39
Autumn	26.91	26.83	26.55	26.54
Annual	42.75	42.97	42.21	41.99

**Table 8.** Monthly, seasonal, and annual variations for parameters of distributions.

Goodness of fit test	Burr (4P)		Gen. gamma		Weibull	
	$K - S$	$Chi-squared$	$K - S$	$Chi-squared$	$K - S$	$Chi-squared$
	Stats - Rank	Stats - Rank	Stats - Rank	Stats - Rank	Stats - Rank	Stats - Rank
January	0.05307 - 1	58.012 - 3	0.05450 - 2	31.358 - 2	0.06804 - 3	28.542 - 1
February	0.05787 - 2	32.985 - 2	0.08246 - 3	62.180 - 3	0.05741 - 1	32.445 - 1
March	0.03457 - 1	27.726 - 2	0.04449 - 3	35.124 - 3	0.04151 - 2	18.665 - 1
April	0.04697 - 2	20.897 - 1	0.04486 - 1	21.965 - 2	0.06327 - 3	56.990 - 3
May	0.09331 - 2	49.839 - 1	0.11223 - 3	78.759 - 3	0.08528 - 1	57.473 - 2
June	0.04887 - 1	17.687 - 1	0.12076 - 3	138.17 - 3	0.11040 - 2	137.75 - 2
July	0.04669 - 1	14.438 - 1	0.15418 - 3	215.01 - 3	0.13195 - 2	204.35 - 2
August	0.05288 - 1	52.837 - 2	0.10172 - 3	61.975 - 3	0.06008 - 2	44.683 - 1
September	0.06236 - 1	45.863 - 1	0.12146 - 3	106.67 - 3	0.07685 - 2	85.443 - 2
October	0.04532 - 1	44.136 - 2	0.05931 - 3	40.118 - 1	0.04583 - 2	54.460 - 3
November	0.04528 - 2	19.942 - 1	0.03913 - 1	26.833 - 2	0.04754 - 3	46.605 - 3
December	0.04771 - 1	44.229 - 2	0.08203 - 3	134.60 - 3	0.05907 - 2	43.637 - 1
Winter	0.04111 - 1	44.347 - 1	0.05046 - 3	147.85 - 3	0.04505 - 2	44.985 - 2
Spring	0.04428 - 1	45.411 - 1	0.04632 - 2	48.439 - 2	0.05466 - 3	98.811 - 3
Summer	0.03084 - 1	34.051 - 1	0.12672 - 3	546.19 - 3	0.10961 - 2	402.35 - 2
Autumn	0.04100 - 1	65.919 - 1	0.05017 - 3	68.270 - 2	0.04313 - 2	84.304 - 3
Annual	0.06197 - 1	621.960 - 2	0.07228 - 3	697.53 - 3	0.06576 - 2	587.39 - 1
$R^2$	0.999660 - 1		0.999644 - 2		0.999105 - 3	
$RMSE$	0.02087 - 1		0.0213655 - 2		0.033887 - 3	

followed theoretical CDF values can be seen in Figure 5. Based on SD values of monthly wind speed data, the Burr distribution was more successful between May and September. However, the Weibull distribution performed better during the remaining months. During the winter, the Weibull model had the lowest SD (0.83

m/s); during the summer (the windiest season), the Burr distribution had the lowest SD (1.31 m/s). This situation is illustrated in Figure 6. From this figure, it is clear that if the wind speed increases in the stable weather conditions, the Burr distribution can give the best fit-to-wind speed data. Based on 3 distribution models, 4 different goodness-of-fit tests were applied; the results are given in Table 8. Comparing the suitability test results ( $K - S$ ,  $R^2$ , chi-squared, and RMSE), the best distribution function can be selected according to the highest value of  $R^2$  and the lowest  $K - S$ , chi-squared, and RMSE values. From Table 8, the  $K - S$ , and  $R^2$  values for the Burr distribution are 0.06197 (Rank 1) and 0.999660 while the chi-squared and RMSE values are 621.960 and 0.02087, respectively. The Weibull  $K - S$ , chi-squared,  $R^2$ , and RMSE values are 0.06576 (Rank 2), 587.39, 0.999105, and 0.033887, respectively. According to RMSE and  $R^2$  results, the Burr distribution ensures a close fit throughout the empirical distribution when compared to the other models. As mentioned in section 1, there have been only limited studies in Antakya so far. When our results are compared with the studies conducted by Celik, and Bilgili and Sahin, the assessment process can be divided into 3 parts. In the first part, the descriptive statistics of this study and the results of Celik, and Bilgili and Sahin are similar with respect to the mean values of the data. In the second part, based on wind data fitting procedures, Celik, and Bilgili and Sahin used Weibull and/or Rayleigh distributions and proposed the Weibull distribution in all cases. However, we implemented the untested Burr and generalized gamma models, as well as the tested Weibull, to determine the wind profile of Antakya. We found that Burr had better adaptability than the Weibull model based on goodness-of-fit test values. Finally, concerning mean power densities, the results from the studies by Bilgili and Sahin differed from our own. Their investigations were achieved using the Wind Atlas Analysis and Application Program (WASP). The WASP runs based on wind turbine types. However, details of the turbine used in their study are not given. Therefore, the comparison is not equitable. The results of Celik and our study, on the other hand, are well-matched.

### 3.3. Wind power assessment

In this work, due to the region's wind profile, the small-scale Enercon E-33 (330 kW) wind turbine was selected to estimate power production. The performance evaluation of the turbine was done with the wind data at 50 m HAGL. The turbine was also placed in the same location as the mast to improve the verifiability of the results. The wind turbines characterization results, observed–estimated seasonal energy producing (MWh), and  $C_f$  values can be seen in Figure 7. It is important to underline that, for the 4 seasons, the highest and the lowest energy was produced in summer and winter, respectively, with 233 MWh (33%) and 21 MWh (2%). Choosing the right turbine design and size may support applications requiring less electricity, such as water pumps, battery charging units, and local off-grid consumption.

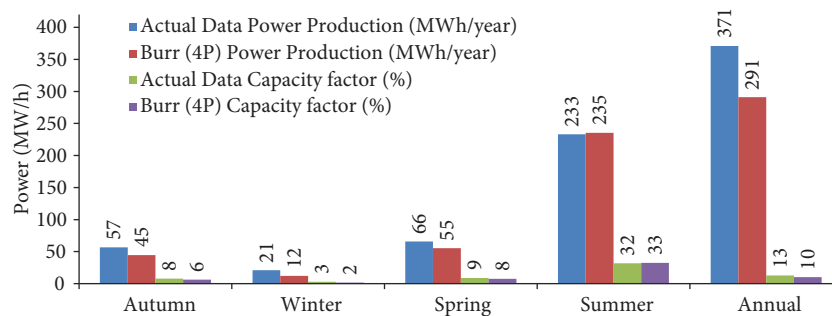


Figure 7. The seasonal power productions and the capacity factors.

#### 4. Conclusions

In this study, wind characteristics of the Antakya region of Hatay Province were statistically analyzed. Performances of the probability models were compared to the measured monthly and yearly wind speed values. The results can be summarized as follows:

- a) The lowest–highest MWS (at 10 m and 50 m HAGL) were 4.39–1.26 and 7.19–2.06 m/s, respectively.
- b) The mean standard deviation of the Burr frequency distribution was about 1.15 m/s for the annual MWS. The values of the Weibull and generalized gamma distributions were 1.25 and 1.28, respectively. The most likely incoming wind directions were northeast ( $45^\circ$ ) and south–southwest ( $202^\circ$ ) throughout the study period.
- c) The Weibull and the generalized gamma distributions need be taken into consideration in the Antakya region. For power production, due to the low SD and best-fitting curve for high wind speeds (see Figure 4), the Burr distribution can be preferred for all seasons.
- d) The highest mean power density value was  $212.46 \text{ W/m}^2$  in August and the lowest average power density was  $5.38 \text{ W/m}^2$  in December (at 50 m HAGL). The best period for wind power production was during the summer months.

These results show that, overall, the potential to generate electricity from wind in Antakya is low; wind power cannot be used alone to meet all the energy needs in the region. However, this study might help to encourage the utilization of small-scale wind energy projects in Antakya, particularly for electrical applications in rural areas, such as traffic warning signs, street lighting, wireless Internet gateways, battery chargers, and water pumps.

#### Acknowledgment

The authors thank the Turkish State Meteorological Service for providing meteorological data.

#### References

- [1] Kose R. An evaluation of wind energy potential as a power generation source in Kütahya, Turkey. *Energy Convers Manage* 2004; 45: 1631–1641.
- [2] International Energy Agency. World energy outlook 2012; November 2012; Paris, France. pp. 532–541.
- [3] Uçak, H. Turkey's population dynamics as a candidate country for EU membership. *International Journal of Economics & Financial Issues (IJEFI)* 2011; 1: 180–198.
- [4] Turkish Electricity Transmission Company (TEIAS). Turkish electricity generation -transmission statistics. Statistical reports 2012.
- [5] Akdağ SA, Önder G. Evaluation of wind energy investment interest and electricity generation cost analysis for Turkey. *Appl Energy* 2010; 87: 2574–2580.
- [6] Global Wind Energy Council (GWEC). Annual Market Update. Global Wind Report 2012; 60–61.
- [7] Turkish Wind Energy Association (TWEA). Turkish Wind Energy Statistics 2013.
- [8] Sahin B, Bilgili M, Akilli H. The wind power potential of the eastern Mediterranean region of Turkey. *J Wind Eng Ind Aerod* 2005; 93: 171–183.
- [9] Sahin B, Bilgili M. Wind characteristics and energy potential in Belen–Hatay, Turkey. *Int J Green Energy* 2009; 6: 157–172.
- [10] Celik AN. A statistical analysis of wind power density based on the Weibull and Rayleigh models at the southern region of Turkey. *Renew Energy* 2003; 29: 593–604.



- [11] Celik AN. On the distributional parameters used in assessment of the suitability of wind speed probability density functions. *Energ Convers Manage* 2004; 45: 1735–1747.
- [12] Gökçek M, Bayülken A, Bekdemir S. Investigation of wind characteristics and wind energy potential in Kırklareli, Turkey. *Renew Energ* 2007; 32: 1739–1752.
- [13] Eskin N, Artar H, Tolun S. Wind energy potential of Gökçeada Island in Turkey. *Renew Sust Energ Rev* 2008; 12: 839–851.
- [14] Ucar A, Balo F. Investigation of wind characteristics and generation potentiality in Uludag-Bursa, Turkey. *Appl Energ* 2009; 86: 333–339.
- [15] Früh W. Long-term wind resource and uncertainty estimation using wind records from Scotland as example. *Renew Energ* 2013; 50: 1014–1026.
- [16] Hensen JLM. Simulation of building energy and indoor environmental quality-some weather data issues. In *Proc. Int. Workshop on Climate data and their applications in engineering*; 4–6 October 1999; Czech Hydrometeorological Institute in Prague, Czech Republic: pp. 4–6.
- [17] Ouammi A, Dagdougui H, Sacile R, Mimet A. Monthly and seasonal assessment of wind energy characteristics at four monitored locations in Liguria region (Italy). *Renew Sust Energ Rev* 2010; 14: 1959–1968.
- [18] WINEUR Reports. Urban Wind resource assessment in the UK: An introduction to wind resource assessment in the urban environment 2007; 9–10.
- [19] Bailey H, McDonald SL. *Wind Resource Assessment Handbook: Fundamentals for Conducting a Successful Monitoring Program*. Albany, NY, USA: Wind Books Incorporated, 1997.
- [20] Hamouda YA. Wind energy in Egypt: economic feasibility for Cairo. *Renew Sust Energ Rev* 2012; 16: 3312–3319.
- [21] Akdag SA, Dinler A. A new method to estimate Weibull parameters for wind energy applications. *Energ Convers Manage* 2009; 50: 1761–1766.
- [22] Genc, A, Erisoglu M, Pekgor A, Oturanc G, Hepbasli A, Ulgen K. Estimation of wind power potential using Weibull distribution. *Energ Source* 2005; 27: 809–822.
- [23] Philippopoulos K, Deligiorgi D, Karvounis G. Wind speed distribution modeling in the greater area of Chania, Greece. *Int J Green Energy* 2012; 9: 174–193.
- [24] Carta JA, Ramírez P, Velázquez S. A review of wind speed probability distributions used in wind energy analysis. *Renew Sust Energ Rev* 2009; 13: 933–955.
- [25] Justus CG. *Physical climatology of solar and wind energy*. Singapore: World Scientific; 1996; AWS Scientific, Inc. pp. 321–76.
- [26] Scerri E, Farrugia R. Wind data evaluation in the Maltese Islands. *Renew Energy* 1996; 7: 109–114.
- [27] Hennessy JP. Some aspects of wind power statistics. *J Appl Meteorol* 1977; 16: 119–128.
- [28] Aidan J, Ododo JC. Wind speed distributions and power densities of some cities in northern Nigeria. *J Eng Appl Sci* 2010; 5: 420–426.
- [29] Seguro JV, Lambert TW. Modern estimation of the parameters of the Weibull wind speed distribution for wind energy analysis. *J Wind Eng Ind Aerod* 2000; 85: 75–84.
- [30] Mathew S. *Wind Energy: Fundamentals, Resource Analysis and Economics*. Berlin, Germany: Springer Verlag, 2006.
- [31] Tsogt K, Zandraabal T, Lin C. Diameter and height distributions of natural even-aged pine forests (*Pinus sylvestris*) in Western Khentey, Mongolia. *Taiwan J For Sci* 2013; 28: 29–41.
- [32] Lo Brano V, Orioli A, Ciulla G, Culotta S. Quality of wind speed fitting distributions for the urban area of Palermo, Italy. *Renew Energ* 2011; 36: 1026–103.
- [33] Abbes M, Belhadj J. Wind resource estimation and wind park design in El-Kef region, Tunisia. *Energy* 2012; 40: 348–357.

- [34] Auwera LV, Meyer F, Malet LM. The use of the Weibull three-parameter model for estimating mean wind power densities. *J Appl Meteorol* 1980;19: 819–25.
- [35] Ghasemi A, Zahediasl S. Normality tests for statistical analysis: a guide for non-statisticians. *J Clin Endocr Metab* 2012; 10: 486–489.
- [36] Elliott DL, Schwartz MN. Wind energy potential in the United States. PNL-SA-23109. Richland, WA: Pacific Northwest Laboratory; September 1993. NTIS no. DE94001667.
- [37] Li M, Li X. Investigation of wind characteristics and assessment of wind energy potential for Waterloo region, Canada. *Energ Convers Manage* 2005; 46: 3014–3033.
- [38] Lima L. Wind resource evaluation in São João do Cariri (SJC)–Paraíba, Brazil. *Energ Convers Manage* 2012; 16: 474–480.
- [39] ENERCON Gmh. ENERCON Gmh technical specs for e-class turbines 2012.